Proceedings of the 8th International Symposium on Transport Phenomena and Dynamics of Rotating Machinery, ISROMAC – 8, Vol. II, March 2000

NUMERICAL STUDY ON ADVANCED INTERNAL COOLING OF GAS TURBINE BLADES WITH RIB TURBULATORS

Kazuya Tatsumi, Hiroshi Iwai and Kenjiro Suzuki
Department of Mechanical Engineering
Kyoto University
Yoshida Honmachi, Sakyo-ku, Kyoto 606-8501,Japan
Fax : 81-75-771-7286, E-mail : tatsum28@htrans.mech.kyoto-u.ac.jp

Kyoji Inaoka
Department of Mechanical and Systems Engineering
Doshisha University
Kyotanabe, Kyoto 610-0321,Japan
Fax : 81-774-65-6802

KEY WORDS: Rib Turbulators, Numerical Analysis, Heat Transfer, Vortices.

ABSTRACT

Many studies have been carried out over turbulent flows in a ribbed channel. However, flow structure and its related heat transfer have not still been clarified in detail. The present study shows a three-dimensional numerical work on full-span ribs and interrupted ribs to investigate the local fluid and heat transfer characteristics. Eventually, the rib having gaps in the spanwise direction generates vortices downstream and showed a higher performance comparing to the full-span rib. Especially, the rib with a gap in the middle is suggested to be best in performance for cooling the duct sidewalls effectively.

INTRODUCTION

Because of its high efficiency compared to those of other power generating systems, advanced gas turbines are considered effective to reduce CO2 emission and therefore to give a remedy for global warming and to save natural energy resources. In order to increase the efficiency of the gas turbine cycle, as is well known, it is necessary to raise the inlet gas turbine temperature, the temperature of the gas flowing into the turbine. On the other hand, a serious fracture problem is caused in the high temperature condition for the materials of gas turbine elements, especially of the turbine blades. The rib turbulators are well known to be effective to enhance the convective heat transfer. Therefore, they are widely used for internal cooling, or for the cooling passage, of the gas turbine blade.

Many studies have been carried out over heat transfer in ribbed channels for various types of ribs. Discrete ribs and V-shaped ribs have been reported to increase heat transfer comparing with the full-span ribs(Lau et al., 1991). Ribs placed in various angles under the condition of rotating channels, have also been studied experimentally(Zhang et al,1994; Dutta et al., 1995). However, the fluid and heat transfer characteristics of turbulated flows with such ribs have not been studied in detail and further research works on those topics are necessary.

To effectively enhance the heat transfer with the rib turbulators, it is important to investigate the structure of flow and related thermal fields in the rib-attached channel. Basically, rib turbulator evokes separation and reattachment of the flow. As is well known, flow reattachment causes noticeable spatial variations of the local heat transfer coefficient. On the other hand, interrupted rib turbulators, which have gaps in the spanwise direction, show a significant difference from the full-span ribs in the characteristics of fluid flow and heat transfer. This is related to the existence of the gaps, by which the secondary flow, such as vortices, are generated downstream the rib. Combination of the flow reattachment effect and the secondary flow effect makes the phenomenon complicated but is worth to analyze in order to establish better internal cooling of gas turbine blades. Furthermore, the ratio of the gap width and the duct width is an essential factor affecting the performance of the interrupted rib in relation with the secondary flow effect mentioned above. For this reason, it should be important to analyze systematically the total performance and the fluid and thermal characteristics of the ribs for various geometry.

In the present study, three-dimensional numerical simulation is carried out for the duct flow with a rib tur-

bulator attached on its bottom wall. The structure of turbulent flow and related thermal fields will be studied and eventually some suggestion will be developed for the improvement of the efficiency of the related heat transfer.

COMPUTATIONAL PROCEDURES

Time-averaged forms of three-dimensional continuity, momentum and energy equations are solved in the numerical computations.

$$\frac{D\rho}{Dt} = -\rho\left(\frac{\partial U_j}{\partial x_j}\right) \quad (1)$$

$$\frac{D\rho U_i}{Dt} = -\frac{\partial P}{\partial x_i} + \frac{\partial}{\partial x_j}\left(\mu\frac{\partial U_i}{\partial x_j} - \rho\overline{u_i u_j}\right) \quad (2)$$

$$\frac{D\rho\theta}{Dt} = \frac{\partial}{\partial x_j}\left(\frac{\mu}{Pr}\frac{\partial\theta}{\partial x_j} - \rho\overline{u_j\theta}\right) \quad (3)$$

For turbulence model, in order to calculate the Reynolds stress in eq.(2), the k-ϵ model proposed by Launder and Sharma(Launder and Sharma, 1974) is adopted. Furthermore, the correction term introduced by Yap(Yap, 1987) is attached into the dissipation equation of this model. In this computation, turbulent heat flux is assumed to be proportional to the temperature gradient, i.e.

$$-\overline{u_i\theta} = \frac{\nu_t}{Pr_t}\frac{\partial\theta}{\partial x_i} \quad (4)$$

Turbulent Prandtl number was assumed to be constant and $Pr_t = 0.9$.

Fully implicit forms of finite difference equivalents of the above mentioned equations were solved numerically along the time axis. For the finite-difference method of the governing equations, a forth-order central-difference scheme was employed for the diffusion terms while the fifth-order upwind scheme was employed for the convection terms in the case of momentum equation. In the energy equation and in the two turbulence transport equations of k and $\tilde{\epsilon}$, a first-order upwind scheme was adopted for the convection terms and a central-difference scheme for the diffusion terms. For the solution algorithm adopted for the pressure equation, SIMPLE algorithm was employed. In order to relax the solutions of the above types of elliptic differential equations, iterative procedure was applied at each time step. In this procedure, alternating direction implicit (ADI) method was also combined.

The computational domains in the present study are illustrated in Fig. 1 together with the coordinate system to be used. Three types of ribs were investigated, which are; (a) a full-span rib (hereinafter referred as FS rib), (b) a rib having gaps at both side ends (hereinafter referred as SG rib) and (c) a rib having a gap at middle(hereinafter referred as MG rib). The origin of the coordinate system is located at the center of the rear bottom corner of the rib. The inlet to the domain was located at about ten rib heights ($10H$) upstream of the front rib surface, where a fully developed turbulent flow was assumed to flow in. Inlet flow conditions were established by a preliminary

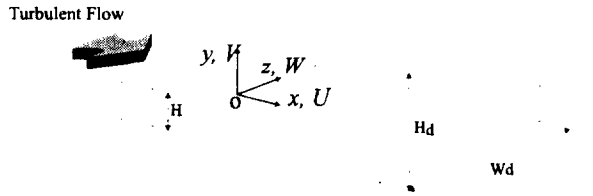

(a) Full-span(FS) rib

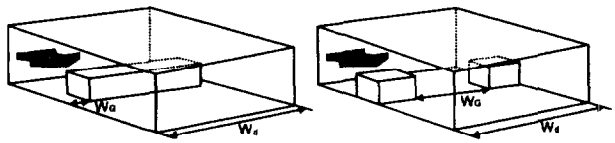

(b) SG rib (gaps at both sides) **(c) MG rib (gap at middle)**

Figure 1 Computational domain.

computation for a 3-D duct flow. The outlet of the computational domain was located at about thirty rib heights ($30H$) downstream the rib, where gradients of all variables (except pressure) in the direction normal to the outlet surface were set equal to zero.

The present investigation was made for three different levels of Reynolds number at 10,000 to 20,000 and parameter study was made for rib width to duct width ratio for the interrupted rib. The gap width to duct width ratios (W_G/W_d) were changed in three style 0.25, 0.2 and 0.15 for SG rib and were 0.5, 0.4 and 0.3 for MG rib. The rib height to duct height ratio (H/H_d) was set equal to 0.15 and the aspect ratio (AR=H_d/W_d) to unity, i.e. a square shaped duct, for all computations.

For boundary conditions at walls, all variables except temperature were set equal to zero. For the thermal boundary conditions, all walls including the rib surfaces were set constant in heat flux through all the computations.

RESULTS AND DISCUSSION

3-D simulations for FS rib

Fundamental characteristics of the two-dimensional flow with a rib turbulator are well discussed and knowledge were acquired for flow separation and reattachment. However, study has not fully been made for the effect of the sidewall, which inevitably exists in the cooling of gas turbine airfoil. In this section, results of 3-D calculations are reported to investigate the three-dimensional effect of the sidewalls on the flow and thermal fields.

For all three conditions of different values of Re, the flow structure showed similarity except that the reattachment location shifts downstream as Re increases in the range from x/H=9.3 to 10.6, if measured at the centerline. Here, the case of Re=20,000 is discussed to demonstrate the local fluid and thermal characteristics of the rib turbulator.

Figures 2 and 3 illustrate the distributions respectively of the skin friction coefficient, C_f and the Nusselt

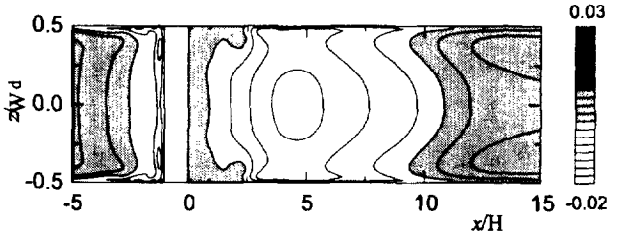

Figure 2 Skin Friction coefficient, C_f at bottom wall. (Re=20,000)

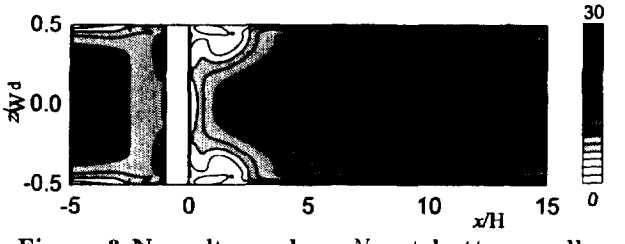

Figure 3 Nusselt number, Nu at bottom wall. (Re=20,000)

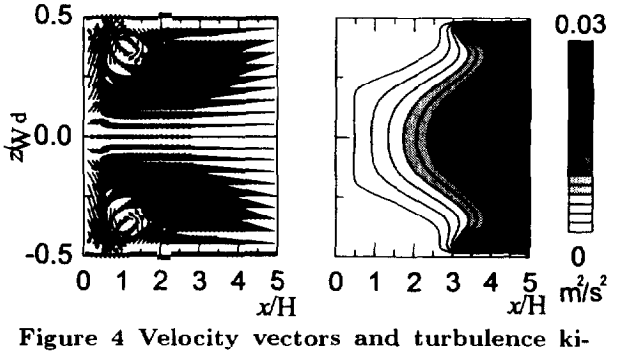

Figure 4 Velocity vectors and turbulence kinetic energy contours near bottom wall. (x-z **plane,** Re=20,000)

number, Nu on the bottom wall of the duct. For C_f, the shaded parts correspond to the area of its positive value while the white parts to its negative value. Three-dimensional effect of the sidewall is observed both in the reattachment region and flow recirculating region both at the front and backside of the rib. Especially for the region just downstream the rib, wall effect is obvious and the local heat transfer shows a distinctive deterioration near the sidewalls. This lower heat transfer performance is caused by the tornado like vertical vortices generated at such positions. Figure 4 shows the velocity vectors and turbulence kinetic energy contours in a plane of y/H=0.03 near the bottom wall. These vortices are produced by the combined effects of the reverse flow in the central region toward upstream from the reattachment point and the downward inclination of the flow passing the rib near its side ends. Kinetic energy of the turbulence is small at the center of these vortices, which causes the low heat transfer efficiency.

3-D simulations for SG rib

Various reports indicated that the interrupted rib turbulators, ribs having gaps at both ends, increase the heat transfer efficiency and total performance (Lau et al., 1991; Balatka et al., 1997). In this section, results of 3-D calculations are reported for the ribs having gaps at both ends under three different conditions of changing the gap width to rib width ratio, i.e. W_G/W_d=0.25, 0.2 and 0.15. Reynolds number was also changed in three steps of Re=10,000, 15,000 and 20,000. Actually, Reynolds number did not show a large influence to the basic flow structure itself except that the position of the

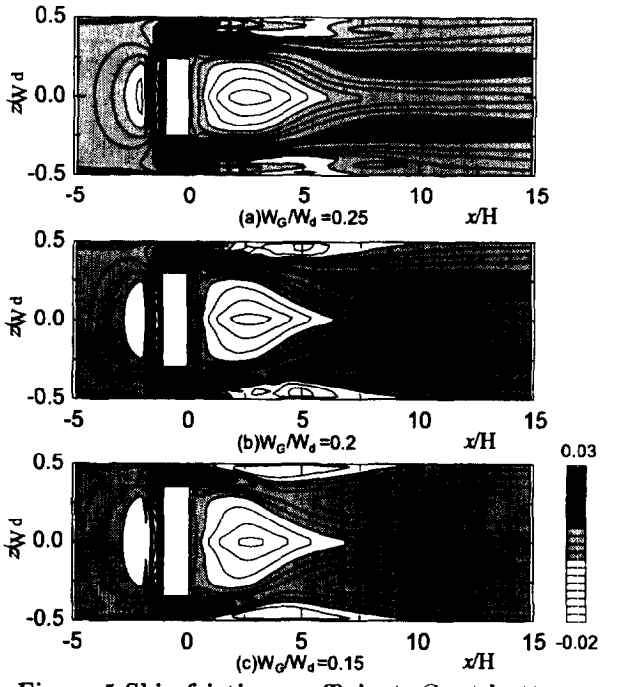

Figure 5 Skin friction coefficient, C_f at bottom wall. (W_G/W_d=0.25, 0.2 **and** 0.15, Re=20,000)

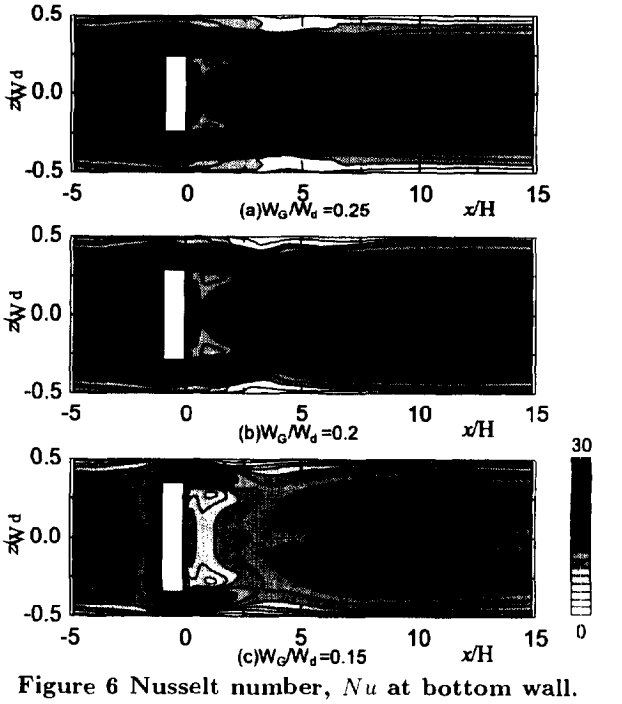

Figure 6 Nusselt number, Nu at bottom wall. (W_G/W_d=0.25, 0.2 **and** 0.15, Re=20,000)

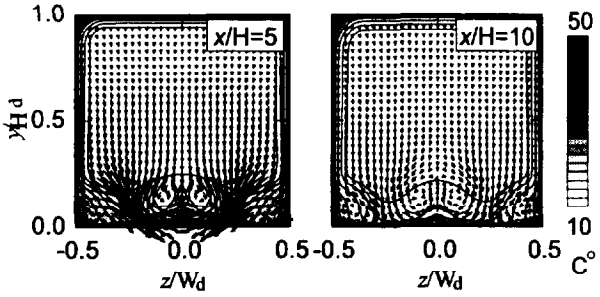

Figure 7 Velocity vectors and temperature contours. (y-z plane, W_G/W_d=0.25, Re=20,000)

reattachment point moved downstream as Re was increased. This was also the case of FS rib. In the case of Re=10,000, unsteadiness appeared in the calculation for each gap width to rib width ratio so that time average value was taken for its results.

Figure 5 and 6 illustrate spatial distribution of C_f and Nu on the bottom wall of the duct for the cases of W_G/W_d=0.25, 0.20 and 0.15 and at Re=20,000. As seen from the comparison with the results for the FS rib, flow and thermal fields differ largely due to the gap existence. The reattachment point is located upstream than that of the FS rib and the size of the recirculation region is reduced. Distribution of Nu is symmetric with respect to the duct centerline. High Nu region elongated streamwisely appears at positions offset from the duct centerline. High heat transfer in this region is produced by the downwash flow appearing in relation with two pairs of longitudinal vortices.

These vortices are observed in Fig. 7 which shows the velocity vectors with temperature contours for the case of W_G/W_D=0.25, Re=20,000 in cross-sections at the locations of x/H=5 and x/H=10. The downwash flows produced by the clockwise vortices conveys the cooler flow from above toward the bottom wall and brings about large value of Nu. Furthermore, anti-clockwise vortices are generated in the corners of the duct. Upwash flows produced by these vortices pump up hot fluid produced by the heated wall. Heat transfer coefficients is found to be smaller there as shown in Fig. 6.

Reverse flows also exist on the duct sidewalls downstream the gaps, where C_f takes negative value, which is indicated by the white parts in Fig. 5. This reverse flow did not appear in the case of FS rib and is related to the flow passing the gaps and to the longitudinal vortices. The height of this reverse flow region was about the same as the rib height. By this reverse flow, the local heat transfer shows deterioration near its area especially on the duct sidewalls. This matter will be discussed in the next section together with the results of FS rib and MG rib.

3-D Simulations for MG Rib

Study is now made for the characteristis of the fluid and thermal fields of the case with a rib turbulator having a gap in the middle. Gap width to duct width ratio has been changed in steps, i.e. W_G/W_d=0.5, 0.4 and 0.3 and the Reynolds number also in three steps of Re=10,000,

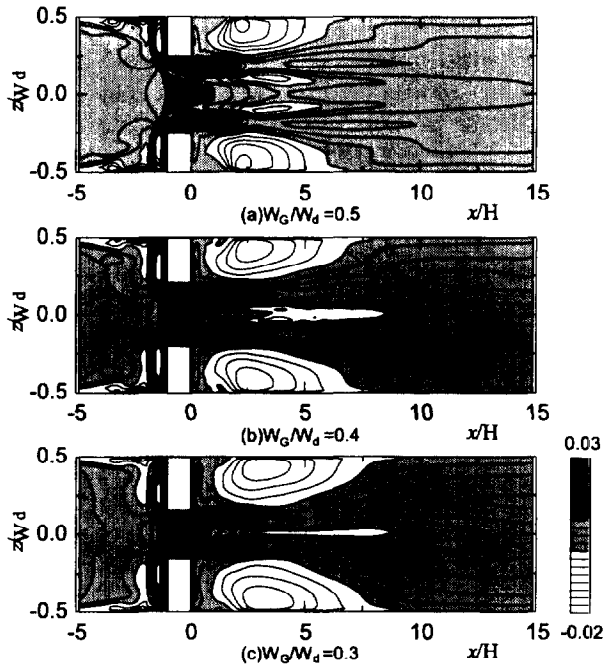

Figure 8 Skin friction coefficient, C_f at bottom wall. (W_G/W_d=0.5, 0.4 and 0.3, Re=20,000)

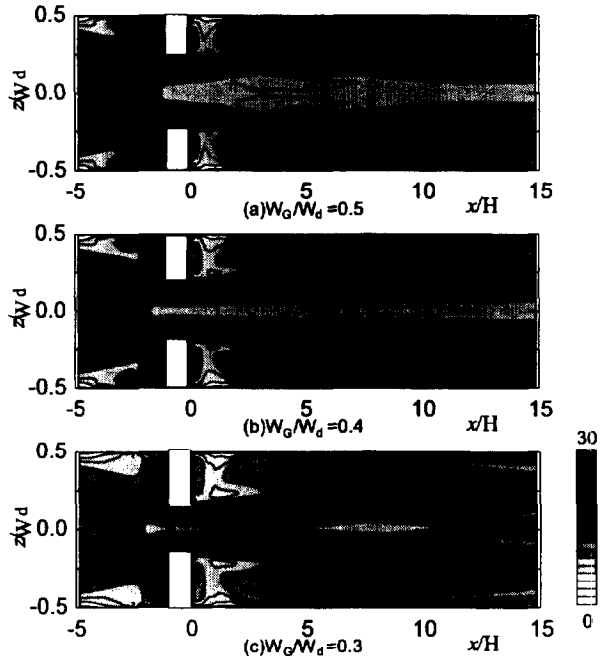

Figure 9 Nusselt number, Nu at bottom wall. (W_G/W_d=0.3, 0.4 and 0.3, Re=20,000)

1,5000 and 20,000. Flow unsteadiness was observed in the low Reynolds number case of Re=10,000. However, if comparing the time average characteristics of flow and thermal fields, difference was found to be small among the three cases of different values of Re.

Figures 8 and 9 show the distributions of C_f and Nu on the bottom wall of the duct for all three cases of W_G/W_d=0.5, 0.4 and 0.3 at Re=20,000. C_f takes negative value in the reverse flow region observed both in front

and behind the ribs. Flow circulation and tornado type vortices appear there. At the position where these vortices sit, low heat transfer occurs due to slow time mean flow and the low kinetic turbulence energy. Reverse flow also appears around the centerline near the duct bottom wall, where C_f takes negative value and Nu smaller value. At the condition of W_G/W_d=0.3, this reverse flow is observed in one single area around the center. However, as the ribs width are reduced and the gap at the center increases, the reverse flow regions appear in a pair on both sides of the centerline.

On the other hand, high heat transfer efficiency is obtained downstream the ribs near the duct sidewalls where downwash flows generated by the vortices exist. Cross-sectional flow structure related to these vortices is shown in Fig. 10 as a velocity vector map superposed with temperature contours at two locations of x/H=5 and x/H=10. It is seen that cooler fluid is directed downwards to the duct bottom surface near the corner region of the duct.

Distribution of Nu on sidewall is shown in Fig. 11 for FS rib, SG rib(W_G/W_d=0.15) and MG rib(W_G/W_d=0.3) for Re=20,000. For FS rib, large value of Nu is observed at several parts downstream the rib along the streamline of the flow passing over the rib edge. On the other hand, low heat transfer efficiency is obtained in a higher region of $y/H_d \geq 0.3$. For SG rib, Nu distribution shows small value near the bottom wall downstream the rib. This low heat transfer performance is related to twofold. First is the warmer upwash flow sweeping the sidewall, which is produced by the counter clockwise vortices located at the bottom corner of the duct. Second is the reverse flow at the duct sidewalls downstream the rib mentioned in the previous section. In the case of MG rib, large Nu distribution is observed in a wide area around and further downstream the rib. This high heat transfer performance downstream the rib results from the downwash flow sweeping the sidewalls produced by the clockwise vortices appearing near the bottom corner of the duct.

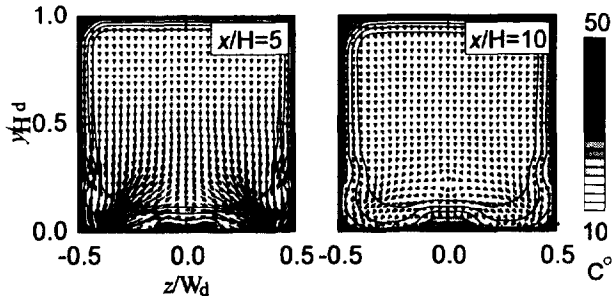

Figure 10 Velocity vectors and temperature contours. (y-z plane, W_G/W_d=0.5, Re=20,000)

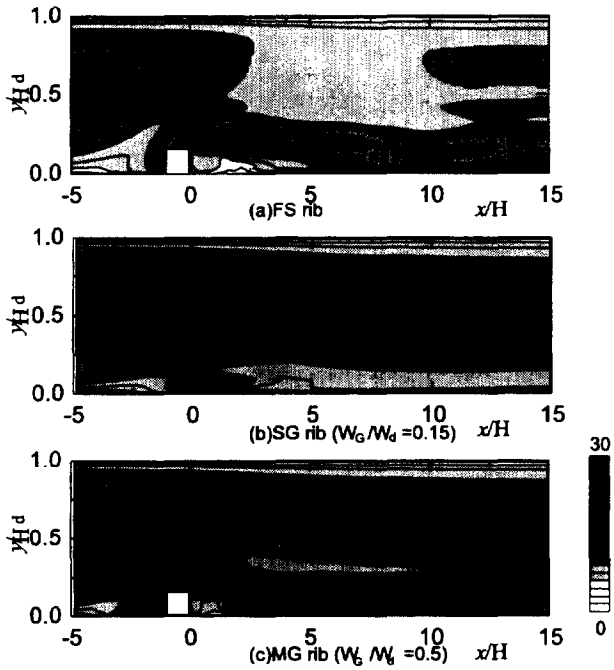

Figure 11 Nusselt number, Nu at sidewall for FS rib, SG rib(W_G/W_d=0.15) and MG rib(W_G/W_d=0.5).

Comparisons of heat transfer efficiency

In the previous three sections, fluid and heat transfer characteristics were investigated for three different kinds of ribs. It is important to make a further study on the total heat transfer efficiency of each rib case to thermally optimize the designing of gas turbine blades.

Figure 12 shows the spatially averaged of Stanton number, S_t for whole surface of the duct and the rib walls in the Reynolds number ranged from Re=10,000 to Re=20,000. Comparing the three different kinds of ribs, it is indicated here that for all Re numbers, MG rib shows the highest heat transfer among the three.

Table 1 shows the spatially averaged value of Nu for all surfaces of the duct and rib walls and the pressure drop coefficient, C_p calculated over the distance between x/H=−5 and x/H=15. Also the efficiency, η calculated by Nu/C_p is indicated in the table and also in Fig. 13. As mentioned above, MG rib shows slightly but distinctively larger Nu value comparing with the other two ribs. This can be explained by comparing the heat transfer coefficient for each divided parts of the duct wall surfaces among the three types of the ribs.

On the bottom wall, especially downstream the ribs, the spatially averaged value of Nu showed a larger value for MG rib than for the other two ribs, FS and SG ribs. The reason of this is twofold. First the vortices generated by the MG rib cover and cool the bottom wall widely. Second by downwash flows produced accompanied with the longitudinal vortices reduces the space of the flow recirculation, where low heat transfer is obtained. At the duct sidewalls, the average Nu there shows a larger value for the MG rib than for the other two ribs. For example, Nu_s=9.2, 9.4 and 11.2 for FS rib, SG rib(W_G/W_d=0.15) and MG(W_G/W_d=0.5) rib at Re=20,000, respectively. This is related to the downwash flow sweeping the sidewalls accompanied with the vortices.

Moreover, considering the C_p and η, interrupted ribs with gaps shows a fairly higher efficiency comparing with

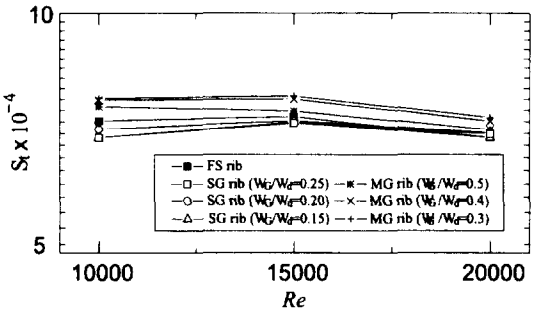

Figure 12 Stanton number, St.

Table 1 : Nu, C_p and η (Re=20,000)

	Nu	C_p	η
FS rib	10.0	3.52	2.84
SG rib (W_G/W_d=0.25)	10.1	0.96	10.5
SG rib (W_G/W_d=0.2)	10.1	1.29	7.83
SG rib (W_G/W_d=0.15)	10.0	1.52	6.64
MG rib (W_G/W_d=0.5)	10.2	0.83	12.7
MG rib (W_G/W_d=0.4)	10.4	1.19	10.2
MG rib (W_G/W_d=0.3)	10.6	1.41	7.5

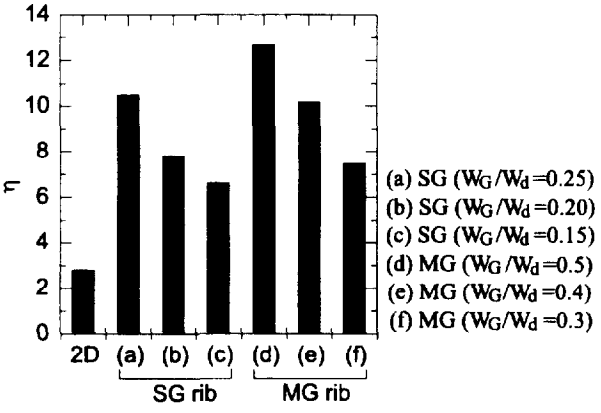

Figure 13 Efficiency, η=Nu/C_p.

the FS rib. This is strongly related to the gap existence where the main flow is possible to pass through.

From the discussions made above, the interrupted ribs show higher efficiency under a constant power or pressure loss comparing with the FS rib. Especially MG rib indicates the largest total heat transfer efficiency. What is more, is that the MG rib is also effective to cool the duct sidewalls and is practically available for cooling air passages in the internal cooling of the gas turbine blades.

CONCLUSION

Three-dimensional numerical computations for a flow over rib turbulators were carried out for the cases of three different kinds of rib geometry. The Reynolds number was changed in the range from Re=10,000 to 20,000 and the gap width to duct width was changed for the ribs having gaps in the spanwise direction. The results obtained from the computations revealed a strong three-dimensionality of flow and thermal fields due to the effect of the duct sidewall. Especially for the ribs with gaps, the flow showed a complicate three-dimensional flow and thermal structure caused by the gaps.

For these interrupted ribs, vortices are generated from the gap side edges and the downwash flow appearing accompanied with vortices increased the heat transfer at the bottom wall and at the sidewalls too for MG rib. The area of flow recirculation region is also reduced by this downwash flow. In this relation, MG rib showed the highest heat transfer efficiency among the three ribs. Considering the pumping power, the interrupted ribs exhibit a fairly efficiency comparing with FS rib.

Nomenclature

H_d, H = duct and rib height, m
W_d, W_G = duct and gap width, m
$AR = \frac{H_d}{W_d}$, aspect ratio
D = duct hydraulic dimater, m
$Re = \frac{\rho U_{ref} D}{\mu}$, Reynolds number
$Nu = \frac{q_w H}{[\lambda(T_w - T_0)]}$, mean Nusselt number
$St = \frac{q_w}{[\rho C_p U_{ref}(T_w - T_0)]}$, mean Stanton number
$C_f = \frac{\tau_w}{(\rho U_{ref}{}^2/2)}$, mean skin friction coefficient
τ_w = wall shear stress, N/m^2
q_w = wall heat flux, W/m^2
T_w, T_0 = wall and inlet Temperature, K
ρ = density of air, Kg/m^2
c_p = heat capacity at constant pressure, J/KgK
λ = fluid thermal conductivity, W/mK
U_{ref} = inlet freestream mean velocity, m/s
Pr_t = turbulent Prandtl number

REFERENCES

Launder, B.E., & Sharma, B.I. 1974, *Letters in Heat Mass Transfer*, Vol. 1, 131-138.

Yap, C.R. 1987, PhD Thesis, Faculty of Technology, Univ. Manchester.

Lau, S.C., McMillin, R.D. and Han, J.C. 1991, Turbulent Heat Transfer and Friction in a Square Channel with Discrete Rib Turbulators, *ASME Journal of Turbomachinery*, Vol. 113, pp. 360-366.

Lau, S.C., R.T., Kukreja and McMillin, R.D. 1991, Effects of V-shaped Rib Arrays on Turbulent Heat Transfer and Friction of Fully Developed Flow in a Square Channel, *International Journal of Heat Transfer*, Vol. 34, No. 7, pp. 1605-1616.

Zhang, Y.M. et al. 1994, Heat Transfer and Friction in Rectangular Channels with Ribbed or Ribbed-Grooved Walls, *ASME Journal of Heat Transfer*, Vol. 116, pp. 58-65.

Duta, S. et al 1995, Influence of Rotation on Heat Transfer from a Two-Pass Channel with Periodical Placed Turbulence and Secondary Flow Promoters, *International Journal of Rotating Machinery*, Vol. 1, pp. 129-144.

Balatka, K., Mochizuki, S. and Murata, A. 1997, Visualization of Three Dimensional Flow around Ribs in a Duct, *The 1st Pacific Symposium on Flow Visualization and Image Processing*, February 23-26, Honolulu, Hawaii.